

TRANSIENT LIQUID PHASE DIFFUSION BONDING OF STAINLESS STEEL 304

M. Mazar Atabaki^{a,b*}, J. Noor Wati^b, J. Bte Idris^b

^a*Institute for Materials Research, the School of Process, Environmental and Materials Engineering, Faculty of Engineering, University of Leeds, Leeds, UK*

^b*Department of Materials Engineering, Faculty of Mechanical Engineering, Universiti Teknologi Malaysia, 81310, Malaysia*

Received 19.08.2011

Accepted 05.04.2012

Abstract

Stainless steel 304 was successfully joined by transient liquid phase diffusion bonding. The bonding process was carried out in a vacuum furnace at various temperatures for various diffusion times, using pure copper interlayer. The joints were studied with optical and scanning electron microscopy (SEM), energy dispersive spectrometry (EDS) and corrosion test. The diffusion of the main elements from the interlayers into the base metal at the bonding temperatures was the main controlling factor pertaining to the microstructural evolution of the joint interface. In order to determine the corrosion resistance of the joints, Tafel test was conducted in 3.5% NaCl solution. The presence of eutectoid γ Fe+ eutectic Cu + Cr was detected at the interface of the joints bonded with copper. The joints related to stainless steel-copper developed crevice corrosion due to galvanic couple between the stainless steel and copper. Pitting was also occurred due to intergranular corrosion on the copper surface.

Key words: Stainless steel; Transient liquid phase diffusion bonding; Characterization.

Introduction

Austenitic stainless steels have been widely used in conventional and nuclear power plants for different applications such as superheaters and heater components; they are also developed for use in cryogenics. These steels also perform well at elevated temperatures and they are extensively used for steam pipes and exhaust systems. The resistance to elevated temperature, oxidation, and corrosion makes the stainless steel a choice for storage tanks. However, there are many difficulties in joining of this material using the fusion welding methods. A concern, when welding the austenitic stainless

* Corresponding author: Mehdi Mazar Atabaki pmmmaa@leeds.ac.uk

steels, is the susceptibility to solidification and liquation cracking [1]. Copper does not form brittle intermetallic compounds with iron and the melting point of the copper is lower than Fe and Ni. Thus, the flow-ability increases at higher temperature and encourage a suitable contact between the faying surfaces [2]. In many instances the formation of brittle intermetallic phases in the diffusion zone leads to unfavorable changes in the mechanical and physical properties of the bonds [3].

The present research focuses on the transient liquid phase diffusion bonding of stainless steel 304 using copper interlayers. The bonding variables and their effect on microstructural changes and mechanical properties of the joints have been investigated using optical and scanning electron microscopy (SEM) and energy dispersive spectrometry (EDS) elemental analyses.

Experimental

The stainless steel 304 was received in the form of 2 mm thick plate. For the bonding process, the plates were cut using abrasive cutting saw to the dimensions of $2 \times 10 \times 20$ mm. The mating surface of the stainless steel was prepared by conventional grinding on 1200 grade SiC paper followed by polishing using diamond paste. The specimens were cleaned in an ultrasonic bath using acetone for 15 min and dried in air. The copper foil (50 μ m thick, 99.95% purity) was used as intermediate material. The bonding process was performed in a vacuum furnace and the substrates and interlayer contact was enhanced by a pressure of 0.5 MP at a set of bonding temperatures. The bonds were prepared at 900, 950 and 1000 °C for 16, 20 and 72 min. Specimens for the metallographic examination were prepared by grinding on 240 to 2400 grade SiC paper and polished the cross section, then etched using 2g FeCl₃, 24 ml distilled water and 6 ml HCl. Microstructural observations were conducted using optical microscope (Nikon microphot-FXL), scanning electron microscope (SEM, PHILIPS XL 40) and energy dispersive spectrometry (EDS). The corrosion test was carried out on the joints in 3.5% NaCl solution in order to determine the corrosion resistance of the bonds in the service condition.

Results and discussion

Microstructural analysis

Figs. 1 a-c show the optical microstructure of the bonded assemblies at 900, 950 and 1000 °C for 20 min holding time, respectively.

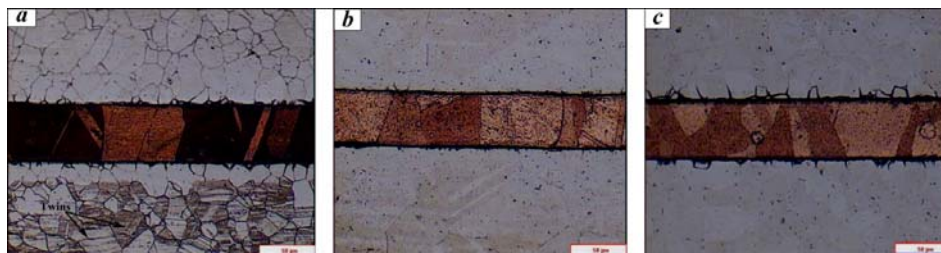


Fig. 1. Optical microstructure of the joints prepared at (a) 900; (b) 950 and (c) 1000 °C for 20 min holding time, using copper interlayer.

It is observed that certain amount of diffusion occurs between the interlayer and substrate. A thin diffusion layer was revealed parallel to the bond interface on the stainless steel side for all bonds.

The interface of the stainless steel and copper consisted of a continuous reaction layer is free from voids at both sides. It is observed that the copper side shows absence of any diffusion layer. SEM images of the joints at 900, 950 and 1000 °C for 20 min holding time are given in Figs. 2 a-c, respectively.

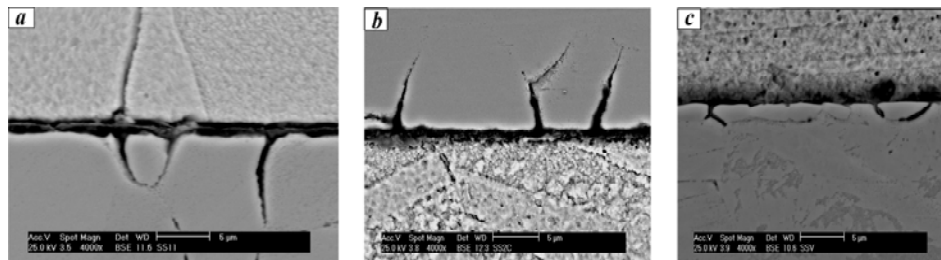


Fig. 2. SEM-BSE images of the joints prepared at (a) 900; (b) 950 and (c) 1000 °C for 20 min holding time.

The crack-shape microstructure in the images shows a diffusion path in the opened grain boundaries of the stainless steel at the faying surface of the interlayer where the interaction of the alloying elements and Gibbs energy is in the highest level at the bonding temperature. In order to determine the chemical composition of the bonding interface, EDS analysis were performed using ‘spot analysis’ taken from stainless steel and copper interlayer. From the observations, various reaction layers were found in the bond zone and base metal and they can be classified in terms of the shape and location of each phase.

The bond area for the joints prepared at 1000 °C can be divided into three distinct zones, which are base metal, diffusion zone and interlayer as shown in Fig. 3.

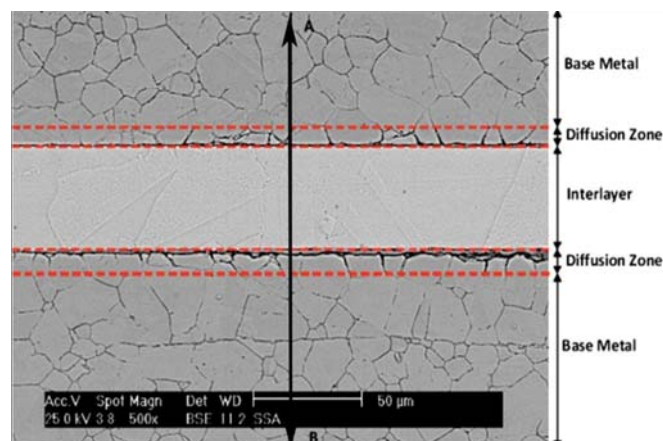


Fig. 3. Three distinct zones in the bonds, showing the solute infiltrated to the grain boundaries of the base metal in the diffusion zone.

Compositional profiles indicating the distribution of the alloying elements from the base metal and interlayer in the centerline shown as AB in Fig. 3 for the specimens bonded at 900, 950 and 1000 °C are presented in Fig. 4.

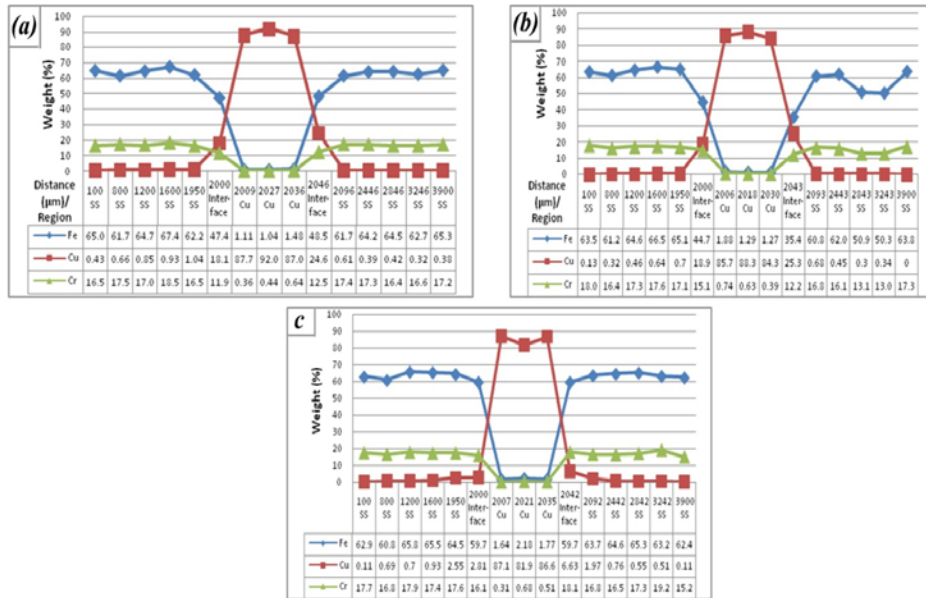


Fig. 4. Elemental distribution of the joints bonded at (a) 900; (b) 950 and (c) 1000 °C for 20 min holding time.

Different rate of elemental distribution like the distribution of Fe, Cr and Cu along the bond area is due to different diffusion coefficients. At the interlayer, the side of which is rich in Cu, however, small amount of diffusion of Fe and Cr occurred from the base metal. It can be clearly seen that the weight percent of Fe and Cr in the interlayer significantly decreases while the weight percent of Cu considerably increases in the base metal.

The decreasing of Fe at the interface is due to dissolution of the base metal. To further analyze the distribution of Fe from the base metal to the interlayer and Cu from the interlayer to the base metal, Cu-Fe binary phase diagram was applied for describing the effect of the melting point depressant on the mechanism of the bonding process [4]. A very low amount of Fe was detected in the copper interlayer due to limited solubility of Fe in copper at the temperature range of 900 to 1000 °C. The copper started to dissolve a little amount of Fe at the stainless steel/copper interlayer interface and continuously diffuses into the interlayer.

The diffusion of Cu into the stainless steel produces a solid solution in a very limited solubility. In addition, the solubility of Cu in Fe was enhanced when the bonding temperature was increased. It can be assumed that the diffusion layer at the bond zone consists of $\gamma\text{Fe} + (\text{Cu})$.

Widening of the Diffusion Zone

The diffusion zone was widened during the bonding operation. The mechanism of the diffusion zone widening is studied by measuring the thickness of the diffusion layer at both sides of the interlayer with initial thickness 50 μm . Table 1 shows the average thickness of the diffusion zone in the stainless steel at 900, 950 and 1000 $^{\circ}\text{C}$ for various holding time. The morphology of the diffusion zone was non-uniform therefore thickness measurements were taken at three different locations of the diffusion zone to have an estimation of average thickness. Obviously, the thickness of the diffusion zones in the stainless steel and copper is increased with increasing the holding time. Mass transfer has to be extended, depending on the bonding temperature. As can be seen, increasing the bonding time and temperature has considerable effect on the interlayer thickness. By increasing the bonding temperature more number of atoms migrated across the interface, hence the reaction layer widened considerably. By approaching to the melting temperature of Cu interlayer, 900-950 $^{\circ}\text{C}$, Cu atoms were stimulated to move faster and in larger quantity. Therefore, it is enough for Cu atoms to vibrate and give possibility to Fe and Cr atoms to diffuse in the interlayer.

Table 1. Average layer thickness in the joints prepared at 900, 950 and 1000 $^{\circ}\text{C}$ for various holding time.

Temperature	$^{\circ}\text{C}$								
	900			950			1000		
Time (min)	16	20	72	16	20	72	20	72	
Thickness									
T_1 (μm) – Diffusion zone	9.286	9.657	15.15	10.013	14.8	16.385	7.581	7.854	
T_3 (μm) – Diffusion zone	7.996	8.664	11.91	6.257	9.748	13.895	7.957	8.432	
T_2 (μm) - Interlayer	47.129	46.933	46.05	45.113	43.357	43.24	42.355	41.121	

Corrosion Test Result

Figs.5 a-c show the optical microstructure of the joints prepared at 900, 950 and 1000 $^{\circ}\text{C}$. Black film deposits were present along the copper surface for all joints. Chloride ions are very aggressive ions to copper and its alloys, due to the tendency of the chloride ion to form an unstable film (CuCl and CuCl_3^{2-}) [5]. Thus, even trace amounts of chloride ions can cause corrosion problem to the interlayer. Fig. 6 shows polarization curve for the joints treated at 900 $^{\circ}\text{C}$ for various holding time.

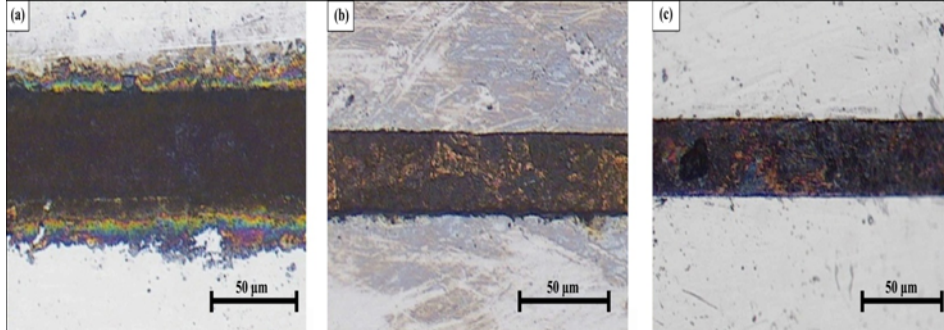


Fig. 5. Optical microstructure of the joints bonded at (a) 900, (b) 950 and (c) 1000 °C for holding time 20 min.

Fig. 6 shows polarization curve for three different temperatures at 20 min holding time for clear observation of each temperature at constant holding time.

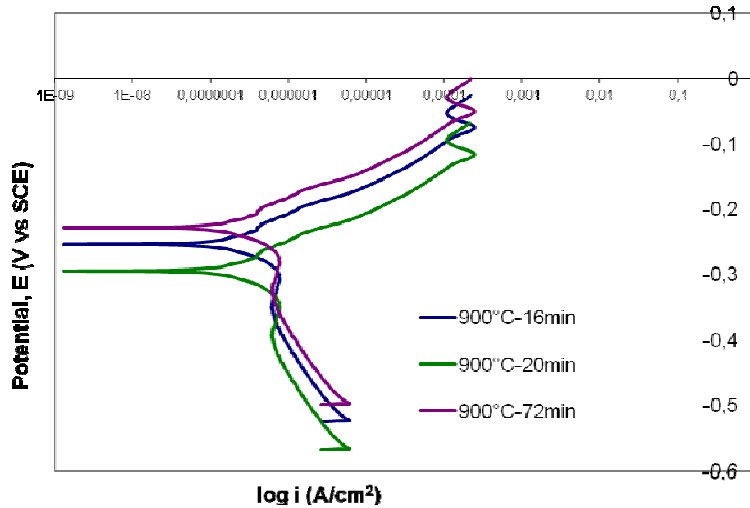


Fig. 6. Tafel curve of the joints bonded at 900 °C for three different holding times.

Fig. 6 shows polarization curve for three different temperatures at 20 min holding time for clear observation of each temperature at constant holding time.

From general observation, it was found that all the joints show same behavior of polarization curve within each temperature due to uniform and continuously bonding contact. Besides, optical examination indicated corrosion attack along the stainless steel-copper interface and copper side. The free corrosion potential (E_{corr}) becomes more negative at lower holding time. Moreover, by reducing the bonding temperature from 1000 to 900 °C, cathodic hydrogen reactions are reduced and E_{corr} increases negatively (see Fig.7).

This statement was shown in detail in Figs. 8 and 9, showing change of E_{corr} as a function of the holding time and the bonding temperature.

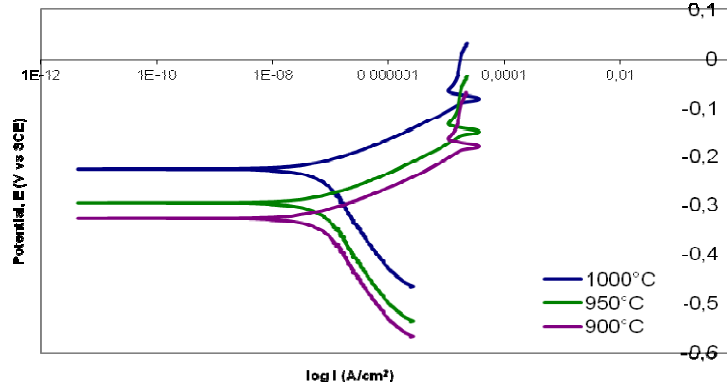


Fig. 7. Tafel curve of the joints prepared at three temperatures for 20 min holding time.

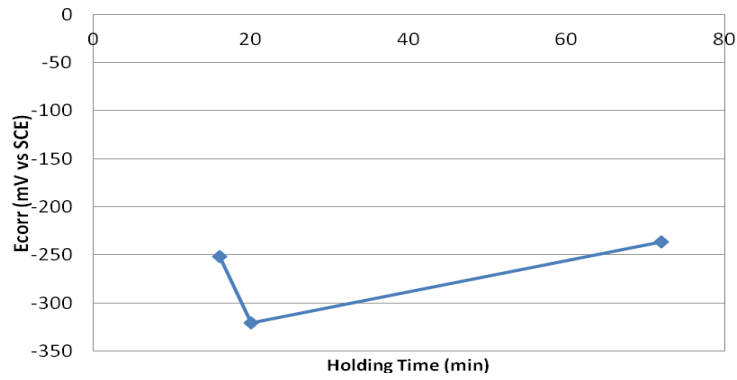


Fig. 8. Corrosion potential as a function of holding time for the bonds prepared at 900 °C.

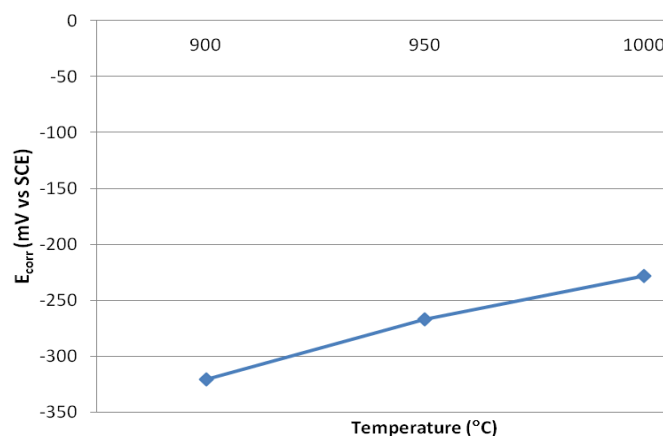


Fig. 9. Corrosion potential as a function of different temperature for the specimens bonded for 20 min holding time.

The corrosion potential of the joints treated at longer holding time and higher temperature is nobler than at shorter holding time and lower bonding temperature. Anodic polarization curve for all joints at the beginning of the test shows that the current density significantly increases from free corrosion potential (E_{corr}) due to dissolution of electrodes at the beginning of the anodic polarization and then the current density decreases due to the passivation of the electrode. At the passivation region, the joint surface is covered with passive oxide film. Then, we can see that the current density starts to increase suddenly due to breakdown of the passive layer (transpassive) until the end of the polarization curve. Transpassivation occurs because some of chemical species in the original passive film turn into higher valence and more soluble products [6]. SEM-BSE examination of the transition joints were performed at the bond line after Tafel test and immersing in 3.5% NaCl solution for 12 h at room temperature. Immersion of the joint was performed in order to determine the open circuit potential (OCP). Open circuit potential is a steady-state or equilibrium potential of an electrode in the absence of the external current flow from the electrode.

Figs. 10 a, b show SEM images for the joints prepared at 900 °C for 22 min after Tafel test without immersing in the 3.5% NaCl solution and after Tafel test with immersing in 3.5% NaCl solution for 12 hours, respectively. As mentioned, the corrosion attacks mostly along the stainless steel-copper interface and inside the copper region. At the anodic polarization curve, the current density was significantly increased for all the joints which is due to dissolution of some phases ($\gamma\text{Fe} + \text{eutectic Cu} + \text{Cr}$), present along the interface which would result in preferential localized corrosion.

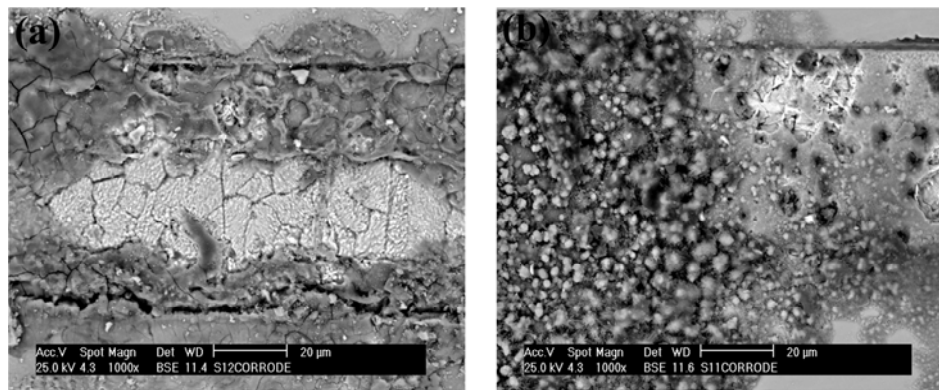


Fig. 10. SEM images of the joints (a) after Tafel test without immersing in the 3.5% NaCl solution and (b) after immersion in 3.5% solution for 12 h then proceed with Tafel test.

Figs. 10 a and 10 b show severe corrosion attack with wide opening (trench formation) at the interface which may be attributed to the dissolution of the phases and the galvanic corrosion. The crevice could be formed after dissolution of the phases ($\gamma\text{Fe} + \text{eutectic Cu} + \text{Cr}$) along the stainless steel-copper interface. Crevice corrosion will develop in all the joints and preferential dissolution of the copper interface was favored during polarization. Stainless steel-copper joint will promote extensive corrosion

between stainless steel and copper inducing a sufficiently different galvanic potential with the metal with the more active potential serving as anode by referring the galvanic series in seawater [7].

On the other hand, galvanic reaction generally causes a reduction in the corrosion rate of the cathodic member of the couple [6]. In this case, stainless steel is more positive than copper so when stainless steel is in contact with copper, the copper will corrode first. The rate of galvanic attack is governed by the size of the potential difference. Referring to the joints, the surface area of the stainless steel is bigger than that of copper. Stainless steel has a large surface area in contact with the electrolyte, while the sacrificial copper has very small surface area in contact with 3.5% NaCl solution; therefore, the stainless steel will generate a large corrosion current, concentrating at a small area of sacrificial copper. Thus, copper corroded firstly and finally stainless steel will be oxidized. The larger the area of the stainless steel, the greater is the acceleration of the copper corrosion. At the copper side, chloride ions were very aggressive, due to their tendency to form an unstable film (CuCl) and soluble chloride complexes (CuCl_2^- and CuCl_3^{2-}). Besides, intergranular corrosion cracking was also found at the copper surface. It is due to interdiffusion of Fe and Cr element along the copper grain boundary and also to formation of Fe-Cr intermetallic phase. This phase dissolves into ($\gamma\text{Fe} + \text{eutectic Cu} + \text{Cr}$) along the interface. Fig. 10 b shows pitting attack on the surface of the copper. Generally, grain boundaries, inclusions such as (sulphides, oxides and nitrides) and local segregation of the alloying elements can act as irregularities, initiating the pitting corrosion. It can be declared that the main alloying elements such as Cr, Ni, Mo and N were segregated into the copper interlayer. Pitting corrosion attacks and propagates easily where Cr and Mo contents are locally depleted forming microsegregations, precipitation of carbides and the formation of intermetallic phases. Meanwhile, for the joints without immersion test, there was no pitting attack found on the copper surface, as this can be seen in Fig.10 a.

Conclusions

Transient liquid phase diffusion bonding was applied to join stainless steel using copper interlayer. Bonding was carried at 900, 950 and 1000 °C for 16, 20 and 72 min in a vacuum furnace. The characterization of the bonds leads to the following findings:

1. The microstructure studies revealed that $\gamma\text{Fe} + \text{eutectic Cu} + \text{Cr}$ accumulated along the diffusion zone. The diffusion zone for the joints increases with increasing temperature and holding time except for the case of the highest bonding temperature (1000 °C) which the changes was not significant.
2. After bonding, the bond region consisted of three distinct zones including parent metal, diffusion zone and diffusion affected zone. There were no eutectic structures in the bond area and a relatively uniform distribution of the alloying elements across the joints occurred, especially at the higher bonding temperature.

The joints developed crevice corrosion due to a galvanic couple formed between stainless steel and copper interlayer and presenting preferential dissolution of copper interlayer under anodic polarization in 3.5% NaCl solution at room temperature. Intergranular corrosion was also found in the copper region. After immersing the joints for 12 hours, pitting attack appeared at the copper surface.

References

- [1] N. Orhan, T. I. Khan, M. Eroglu, *Scripta Mater.* 45 (2001) 441-446.
- [2] M. Mazar Atabaki. *Journal of Nuclear Materials*, 406(3) (2010), 330-344.
- [3] S. K. Mannan, V. Seetharaman and V. S. Raghuthan, *Mater. Sci. Eng.* 60 (1983) 79-86.
- [4] C.W. Sinclair, G.R. Purdy, J. E. Morral, *Metall. Trans. A.* 31 (2000) 1187-92.
- [5] C. W. Yeow, D.B. Hibbert and J. Galvanostatic, *Electrochem. Soc.* 130(1983) 786-90.
- [6] R. Winston Revie and H. H. Uhlig, *Corrosion and Corrosion Control*, Wiley-Interscience, 2008.
- [7] N. Bhuvaneshwaran, U. K. Mudali, P. Shankar, *Scripta Materialia* 49 (11) (2003) 1133-1138.